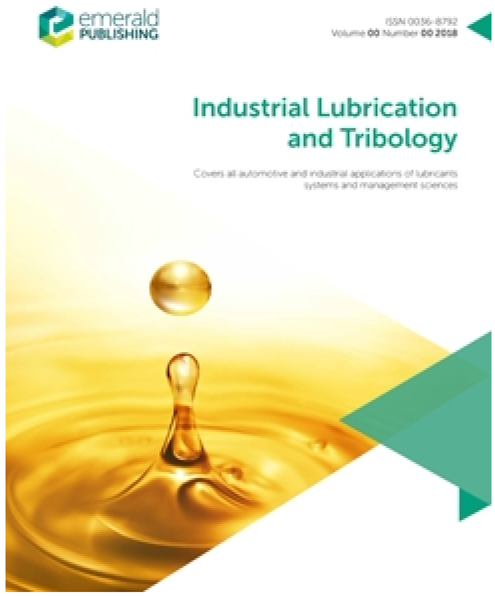


# Effect of plastic pyrolytic oil and waste cooking biodiesel on tribological properties of palm biodiesel-diesel fuel blends


| | |
|---|---|
| Journal: | *Industrial Lubrication and Tribology* |
| Manuscript ID | ilt-08-2021-0338.R3 |
| Manuscript Type: | Original Article |
| Keywords: | Lubricity, Plastic pyrolysis oil, Waste cooking biodiesel, HFRR, Wear and Friction, Palm biodiesel |
| | |

# Effect of plastic pyrolytic oil and waste cooking biodiesel on tribological properties of palm biodiesel-diesel fuel blends

**Purpose** - The purpose of this work was to investigate the lubricity of palm biodiesel (PB)-diesel fuel with plastic pyrolysis oil (PPO) and waste cooking biodiesel (WCB).

**Design/methodology/approach** - Three quaternary fuels were prepared by mechanical stirring. B10 (10% PB in diesel) fuel was blended with 5, 10, and 15% of both PPO and WCB. The results were compared to B30 (30% PB in diesel) and B10. The lubricity of fuel samples was determined using high frequency reciprocating rig (HFRR) in accordance with ASTM D6079. The tribological behavior of all fuels was assessed by using scanning electron microscopy (SEM) on worn steel plates to determine wear scar diameter (WSD) and surface morphology. The reported wear scar diameter (WSD) is the average of the major and minor axis of the wear scar.

**Findings** - The addition of PPO and WCB to B10 had improved its lubricity while lowering wear and friction coefficients. Among the quaternary fuels, B40 showed the greatest reduction in coefficient of friction and WSD, with 7.63 and 44.5% respectively when compared to B10. When compared to B30a, the quaternary fuel mixes (B40, B30b, and B20) exhibited significant reduction in WSD by 49.66, 42.84, and 40.24%, respectively. Among the quaternary fuels, B40 exhibited the best overall lubricating performance, which was supported by surface morphology analysis. The evaluation of B40 indicated a reduced adhesive wear and tribo-oxidation, as well as a smoother metal surface, as compared to B20 and B30b.

**Originality/value** - Incorporation of PPO and WCB in PB-diesel blend as a quaternary fuel blend in diesel engines has not been reported. Only a few researchers looked into the impact of PPO and WCB on the lubricity of the fuel.

**Keywords:** Lubricity; Plastic pyrolysis oil; Waste cooking biodiesel; HFRR; Wear and friction; Palm biodiesel; Diesel

Abbreviation

| | |
|---|---|
| COF | : Coefficient of friction |
| FAME | : Fatty acid methyl ester |
| GC-MS | : Gas chromatography-mass spectrometry |
| HC | : Hydrocarbon |
| HFRR | : High frequency reciprocating rig |
| LDPE | : Low-density polyethylene |
| NaOH | : Sodium hydroxide |
| PB | : Palm biodiesel |

PPO : Plastic pyrolysis oil

SEM : Scanning electron microscopy

USLD : Ultra-low sulphur diesel

VI : Viscosity index

WCB : Waste cooking biodiesel

WCO : Waste cooking oil

WSD : Wear scar diameter

## 1. Introduction

Renewable, clean, and sustainable alternative fuels have become more important as mineral supplies are drained, global warming worsens and environmental challenges intensify (Sudrajat *et al.*, 2020). Up to 30% biodiesel with diesel fuel is used in several regions of the world without any adjustments to the diesel engine. Currently, Indonesia and Malaysia are using B10 (10% palm biodiesel (PB) in diesel) and B20 (20% PB in diesel) fuels successfully, with Indonesia is planning to deploy B40 (40% PB in diesel) by 2022 (Elisha *et al.*, 2019). Malaysia is expected to deploy B30 (30% PB in diesel) by 2025 (Latiff, 2020). The use of PB-diesel blend as a fuel reduced engine performance while improving exhaust gas emissions, except for nitrogen oxides (Ali *et al.*, 2016). Several studies used various alternative fuels (such as waste vegetable oil-based biodiesel and pyrolysis oil) in diesel to improve engine characteristics.

In pyrolysis oils, plastic pyrolysis oil (PPO) outperformed diesel in terms of engine performance and exhaust gas emissions (Kaewbuddee *et al.*, 2020; Sachuthananthan *et al.*, 2018). PPO's brake thermal efficiency and brake-specific fuel consumption were both greater than diesel (Kaewbuddee *et al.*, 2020; Sachuthananthan *et al.*, 2018). PPO produced less hydrocarbon (HC) emission than diesel (Kalargaris *et al.*, 2017). Whereas some researchers combined waste vegetable oil-based biodiesel with diesel as a substitute fuel to achieve better diesel engine performance while lowering emissions (Abed *et al.*, 2018; Al-Dawody *et al.*, 2019; Gad *et al.*, 2021). Waste cooking biodiesel (WCB) has been identified as a viable alternative fuel for reducing engine exhaust gas emissions (Abu Jrai *et al.*, 2011; An *et al.*, 2013).

Fuel lubricity is an important aspect to consider when it comes to the durability of diesel engine components. To comply with the Kyoto Protocol's objective of reducing greenhouse gas emissions, many countries have begun to utilize ultra-low sulphur diesel (ULSD). Compared to petroleum diesel, ULSD possesses poor lubricity. Engine parts rust or are damaged as a result of insufficient lubrication provided by ULSD fuel during fuel injection and pumping.

In addition to emitting fewer pollutants, biodiesel has high intrinsic lubricity (Gopal *et al.*, 2018). Because biodiesel contains 98% methyl ester, it considerably reduces wear and friction when is mixed with petroleum diesel (Wadumesthrige *et al.*, 2009). According to Fazal *et al.* (2013), the coefficient of fraction (COF) values of PB-diesel blends (B10 and B20) and neat PB were 1.83, 2.96, and 4.93% lower than diesel. In contrast to diesel, their wear scar diameter (WSD) values were found to be 1.34 (B10), 9.41 (B20), and 22.72% (B100; 100% PB) lower. As the percentage of PB in secondary fuel blends increased, the COF and WSD decreased.

However, PB has been observed to be prone to oxidation, which can have a negative impact on lubricity. In their study, Awang *et al.* (2021) found that PB had the highest COF. The oxidation process converts the esters into fatty acids such as formic acid, acetic acid, propionic acid, caproic acid, and others (Fazal *et al.*, 2013). PB's polyunsaturated fatty acids, such as oleic acid, could be the most significant component influencing auto-oxidation. Furthermore, adding 10% PB to PPO has raised its COF and WSD by 5.61 and 11.75%, respectively. The oxidation process can result in fuel degradation, reduced lubricity, increased corrosion, and material deterioration (Fazal *et al.*, 2013).

Using the high frequency reciprocating rig (HFRR) based on ASTM D6079 standard, Awang *et al.* (2020) investigated the impact of adding low-density polyethylene (LDPE) waste-based PPO to diesel on the lubricity of the blended fuel. They discovered that adding PPO to diesel lowered COF and WSD, with the least reductions of 17.62 and 19.92%, respectively for 10% PPO in diesel. According to Awang *et al.* (2021), polypropylene and polyethylene waste-based PPO had a lower WSD than B10 by 5.80%, although its COF was 5.44% higher. As a result, PPO could be a suitable component in PB-diesel blend to improve lubricity.

There have not been any investigation on the lubricity of WCB in diesel at different percentages. Fatty acid methyl ester (FAME) has been promoted for use in engines to increase the lubricity of diesel engines in numerous studies (Agarwal, 2003; Dhar and Agarwal, 2014; Kulkarni *et al.*, 2007). FAME contents in WCB were 97.71, 98.14, and 98.5 wt%, according to Mohamed *et al.* (2020), Yusuff *et al.* (2021) and Gardy *et al.* (2019), respectively. Because of the large amount of FAME in WCB, it can be added to diesel as a lubricant.

Plastic waste and waste cooking oil (WCO) are superior alternatives to be converted into fuel and blended with PB and diesel to make B30 blend due to their cost-effectiveness and high availability (Antelava *et al.*, 2019; Czajczyńska *et al.*, 2017; Moecke *et al.*, 2016). According to the literature, PPO and WCB are viable alternative fuels in the B10 diesel, which can improve lubricity. Despite this, certain PPO's poor quality, such as low viscosity, could limit its use in diesel engines at high percentages. To improve such poor fuel qualities, WCB with FAME at greater viscosity is an essential option to be employed with PPO in B10 diesel. The influence of PPO and WCB on the lubricity of PB-diesel blends (B10) is investigated in this study. Tribological behavior was observed for quaternary blends (PPO-WCB-PB-diesel-fuel) for the durability of diesel engines, pumps, and fuel injectors. The lubricity of quaternary fuel mixes was assessed using HFRR, according to the ASTM method (D6079).

During operation, diesel engines' pumps and injectors are lubricated by the diesel fuel itself. There is no report on the incorporation of PPO and WCB in PB-diesel blend as a quaternary fuel blend in diesel engines, according to a review of literature (Abed *et al.*, 2018; Chandran *et al.*, 2019; Singh et al., 2021). Furthermore, only a few studies looked into the influence of PPO and WCB on the lubricity of diesel (Awang *et al.*, 2020; Hu *et al.*, 2016; Sikdar *et al.*, 2020). The lubricity of the fuel is an important factor in determining the longevity of diesel engines. Prior to engine testing, the lubricity of fuel should be determined. During the delivery of diesel fuel into the combustion chamber, the lubricity of diesel injectors is significant.

This research work focuses on the lubricity of PB-diesel fuel with PPO and WCB. The additives have been added in the PB-diesel mixture as a quaternary fuel blend in diesel engines.

It is a very important experimental research work because fuel lubricity is a significant aspect when it comes to durability of diesel engine components. Engine parts rust or are damaged as a result of insufficient lubrication provided by fuel during fuel injection & pumping. The main objective is to minimize adhesive wear and tribo-oxidation due to the presence of polyunsaturated fatty acids in PB that could be the most significant component influencing auto-oxidation. The HFRR test was used to evaluate the lubricity of PB-diesel fuel with PPO and WCB for fuel injector application using a ball-on-plate combination. A ball on a test sample plate was used to evaluate the tribological behavior of fuel samples, in which the steel ball was allowed to slide on a steel specimen while being submerged in fuel sample in a reciprocating motion. The plate scars used in HFFR experiments were analyzed using a scanning electron microscopy (SEM) instrument to study their surface morphology.

## 2. Materials and methods

### 2.1. Materials

PB was purchased from KL-Kepong Oleomas Sdn Bhd and PPO was provided by Syngas Sdn Bhd. WCO from chicken frying was collected from a local restaurant located at Taman Setapak Jaya, Kuala Lumpur, Malaysia. In the current study, WCO was employed as a feedstock in the present study to make biodiesel. AISI 52100 Chrome hard polished steel balls with a diameter of 6.2 mm were brought from SKF Malaysia Sdn Bhd and 15 mm SAE-AMS 6440 steel smooth diamond polish plate was purchased from the local market, according to ASTM D6079.

## 2.2. PPO production

LDPE wastes were gathered and processed into black pellet. The pyrolysis of LDPE black pellet into PPO was conducted via the pyrolysis under the absence of oxygen, the catalytic reforming and the condensation of the resultant gases. A portable semi-batch type reactor was used. Water vapor was used to turn the LDPE black pellet into molten plastic. The molten plastic was heated to a regulated temperature (500 ˚C) in the reactor. The vaporising pressure forced the gas product to flow through the catalytic chamber. The gas product was cracked even more in the catalytic chamber before being vented. Condensation and distillation of the gas product happened after passing through the chamber. After that, the condensed oil (PPO) was stacked in the storage tank. These approaches were adapted from Awang *et al.* (2020).

## 2.3. WCB production

To minimise moisture content, the collected WCO was gradually heated up to 100 ˚C for 10 min. The heated WCO was let to cool down to room temperature before undergoing the filtration process to remove solid particles. Transesterification took place in a glass reactor with a heating jacket that was connected to a heated thermostatic bath, a reflux condenser and mechanical stirrer. To begin, 1000 ml WCO was heated to 60 ˚C. Within this process, 90 g of methanol (30 wt% of WCO) and 3 g of sodium hydroxide (NaOH) (1 wt% of WCO) were mixed into a beaker. Following that, the NaOH pellets were dissolved in methanol to produce a methoxide solution. 300 g of WCO and methoxide solution were mixed with a mechanical stirrer at 830 rpm and heated at 60 ˚C for 1 h to complete the transesterification reaction. After that, the product was placed in a separating funnel and left for 24 h. Two distinct layers of biodiesel and glycerol were formed. The glycerol layer, which was on the bottom, was discarded. Meanwhile, the top layer was rinsed with warm water to obtain the pure biodiesel.

## 2.4. Gas chromatography and mass spectrometry

As described in Table I, the composition of PB, WCB, and B10 diesel was evaluated using gas chromatography-mass spectrometry (GC-MS). After 50 mg of liquid fuel product was dissolved in 1 mL of n-hexane, the sample was injected into the chromatographic inlet and processed for 42 min. The carrier gas is helium, which has a flow rate of 0.51 mL/min. The separation started at a temperature of 50 to 250 °C, with a heating rate of 5 °C/min (Juwono *et al*., 2018). The same method was applied to identify the composition of PPO.

Table I Chemical composition of PB, WCB and B10

***< Insert Table I >***

## 2.5. Fuel samples preparation

To explore the impact of quaternary fuel blends on lubricity properties, three different quaternary fuels (B20, B30b and B40) and a binary fuel (B30a) were prepared. Their composition is shown in Table II. The prepared fuel samples were contrasted to Malaysian diesel that is available commercially (B10). To prepare B30a fuel blend, 20% PB was mixed with 80% B10 diesel (by volume) and agitated for half an hour at 700 rpm until homogeneous. The quaternary fuel blends were prepared by using the same method as B30a fuel. The tested blank fuels and quaternary fuel blends are shown in Figure 1. Table III shows the physicochemical properties of the blank fuels and fuel mixes that were examined.

< ***Insert Figure 1*** >

Figure 1 Tested blank fuels and quaternary fuel blends

Table II The composition of different tested quaternary fuel blends

< ***Insert Table II*** >

Table III Physicochemical properties of tested fuel blends

< ***Insert Table III*** >

### 2.6. Experimental set-up

Eight fuel samples were evaluated using DUCOM's HFFR equipment (Model: TR-281-M8), as indicated in Figure 2. The stainless-steel plates were cut to a dimension of 15 mm × 15 mm to serve as test sample plates, and polished with silicon carbide sheets of 600, 800, 1000, 1500, and 2000 grit on a polishing machine. The plates were then polished with 1 and 3 m diamond suspension as an extra layer of polish. After that, a profilometer (Veeco Dektak 150) was used to measure their surface roughness, which was kept between 0.03 and 0.04 (Ra) on the scale. A ball on a test sample plate was used to evaluate the tribological behavior of fuel samples, in which the steel ball was allowed to slide on a steel plate while being submerged in 2.0 ± 0.2 ml fuel sample in a reciprocating motion. The operating conditions for the tribology test are listed in Table IV below and were based on ASTM D6079, which is the standard test method. The following parameters were maintained: 1.0 ± 0.02 mm stroke length, 50.0 ± 1 Hz frequency for 75 min, 2 ± 0.01 N applied load, and a constant fuel temperature of 25 ± 2 ˚C.

***< Insert Figure 2 >***

Figure 2 Schematic view of reciprocating friction and wear monitor (HFRR) rig

Table IV HFRR tribological test operating conditions

***< Insert Table IV >***

SEM was used to quantify the WSD of worn steel plate after tribological tests. Eq. 1 and 2 below were used to calculate the WSD of worn surfaces and the COF:

$$\mathrm{WSD} = \frac{\mathrm{M} + \mathrm{N}}{2} \qquad (1)$$

in which,

M = major axis (μm) measured through SEM

N = minor axis (μm) measured through SEM

$$\text{COF} = \frac{\text{Actual frictional force (N)}}{\text{Applied Load (N)}} \quad (2)$$

## 2.7. SEM analysis

SEM was used to analyze the surface morphology of worn steel plates after tribological tests. To visualise the type of wear, SEM images were obtained at magnifications of 500, 2000, and 3000×.

# 3. Results and discussions

## 3.1 Chemical composition of PPO, PB, WCB and B10

The fatty acid composition varies depending on the type of biodiesel. Because of the various sources of origin, each biodiesel has its own fatty acid content. In biodiesel, there are two types of fatty acids: saturated and unsaturated fatty acids. Table I showed that saturated acids found in PB include oleic acid and gondoic acid. Unsaturated acids found in PB include caprylic acid, capric acid, lauric acid, myristic acid, pentadecanoic acid, palmitic acid, heptadecanoic acid, arachidic acid and lignoceric acid. Oleic acid has the highest content of fatty acid in PB (48.5%), followed by palmitic acid (34.7%). Meanwhile, saturated acids found in WCB include caprylic acid, capric acid, lauric acid, myristic acid and pentadecanoic acid. Unsaturated acids in WCB include linolenic acid and gondoic acid. WCB contains the highest content of gondoic acid (33.5%), followed by myristic acid (5.2%). Table I also showed that the percentage of unsaturated fatty acid composition is more in PB (49.52%) as compared to WCB (35.94). The biodiesel's unsaturated fatty acid content improves the lubricity of blended fuel. B10 contains 10% POB and 90% petroleum diesel, so its fatty acid content is lower than pure POB. B10 contains 3.32% saturated fatty acids, including 2.1, 0.8 and 0.4% palmitic acid, myristic acid and arachidic acid, respectively.

Table V and Table VI show the chemical composition of B10 and PPO, respectively. B10's GC-MS data reveals that alkanes make up the majority of its chemical components. Alkanes, benzene, naphthalene, and alkenes, respectively, make up 50.0, 5.0, 4.0, and 0.3% of B10. PPO's GC-MS data indicates that it contains alkanes, alkenes, and aromatics. Table VI also reveals that PPO has a lower alkane concentration than B10. This could explain why PPO has lower viscosity than B10, making it suitable for injection with diesel in diesel engines. PPO, on the other hand, has more olefins than B10. PPO has higher benzene level than B10, but lower naphthalene content. PPO can only be used as a mixed fuel with diesel because it has less aromatic components than B10.

Table V GC-MS composition of B10

***< Insert Table V >***

Table VI GC-MS composition of PPO

*< Insert Table VI >*

### 3.2 Physicochemical properties of PPO and WCB in PB-diesel blend

The data were used to evaluate the differences between fuel blends and serve as the basic for comparing the PB-diesel fuel and quaternary fuel, as well as quaternary fuel at different compositions of PPO and WCB. The percentage of PPO and WCB in PB-diesel fuel in each sample is shown in Table II. All of fuel blend properties are listed in Table III.

The density of fuel can provide its composition and nature. The density of quaternary fuels (B20, B30b and B40), mainly HC, varies, between 0.8446 and 0.9449 kg/$m^3$. The densities of B10 and B30a were 0.8482 and 0.8534 kg/$m^3$, respectively.

The VI (viscosity index) of a fuel is a number that represents how viscosity changes with temperature. A low VI indicates a significant variation in viscosity with temperature changes. In other words, at high temperatures, the fuel becomes incredibly thin, whereas at low temperatures, it becomes extremely thick. A high VI indicates that viscosity changes relatively low over a wide temperature range. For the most part, a fuel that maintains a steady viscosity across temperature fluctuations is desirable. When the engine is cold, fuel with the high VI resists excessive thickening, which aids speedy starting and circulation. When the engine's sliding components are hot, it resists excessive thinning, ensuring full lubrication and avoiding unnecessary fuel consumption. The VI is calculated using known viscosity at two different temperatures (in this case, 40 and 100 ˚C). It can be seen from Table III, B30a secondary fuel has a higher viscosity than that of B30b quaternary fuel.

### 3.3 Friction analysis

The COF trend of all evaluated fuel samples over time is shown in Figure 3a. Because there was no lubricating layer between the mating surfaces in the early stages of the experiment, the COF of most samples was high. The running-in period is the first step of the experiment. The surface roughness between the friction surfaces will become smoother over time as a lubricating layer forms between the contact surfaces. The steady-state condition refers to this stage of experiment. The running-in duration for B30a fuel sample is short. The findings show that as the percentages of biodiesel and PPO in the fuel increase, friction decreases. Biodiesel with a higher oxygen content than diesel can help to reduce friction (Wain et al., 2005). Figure 3b shows the average of COF data during running-in state and steady-state for all analyzed samples. The average values of COF for all studied samples (B30a, B40, B30b, B20 and B10) were 0.127, 0.154, 0.155, 0.161 and 0.166, respectively.

***< Insert Figure 3 >***

Figure 3 (a) COF during the run-in period and steady-state period and (b) average COF for all tested fuel samples by HFRR tester

The COF reductions of all studied fuel blends (B30a, B40, B30b, and B20) were 23.89, 7.63, 6.89, and 3.16%, respectively, as compared to B10 diesel. When compared to B10, the B30a fuel mix had the lowest COF due to the higher proportion of FAME, which acts as a protective barrier between the contact (Pehan *et al.*, 2009).

Due to the decrease in viscosity, which has a large influence on the lubricity of fuel, all quaternary fuel blends (B40, B30b, and B20) exhibit an increase in COF of 21.27, 22.34, and 27.25%, respectively, when compared to B30a. Due to the increased biodiesel component (Fazal *et al.*, 2013), which enhances the viscosity of the blend, the B40 has the lowest COF among the quaternary mixed fuels. Furthermore, increasing PPO and WCB concentrations in quaternary blends reduces friction. Fazal *et al.* (2013) made the same observation, stating that COF reduced as biodiesel mix proportions increased. However, COF rose with increasing PPO concentrations, according to Awang *et al.* (2020). In order to validate and better explain the experimental results, similar research was evaluated. Table VII summarizes the COF and WSD derived from this study as well as other research findings. Identical results have been achieved for COF. Biodiesel and PPO improve lubricating properties of diesel fuel, resulting in lower COF than diesel fuel.

Table VII A brief comparison of COF and WSD resulted from present study with other research works

***< Insert Table VII >***

### 3.4 Wear analysis

Figure 4 shows the average WSD of all analyzed samples. All of the samples tested (B40, B30b, B20, B10, and B30a) had WSD values of 1.37, 1.56, 1.63, 2.48, and 2.73 mm, respectively. WSD was reduced by 44.5, 37.0, and 34.1% for B40, B30b, and B20, respectively, as compared to B10. As compared to B10, B30a showed a 9.3% increase in WSD. The different acids produced upon oxidation of esters in PB cause this effect, which is known as oxidative corrosion. Interestingly, as compared to B30a, the quaternary fuel mixes (B40, B30b, and B20) exhibit a reduction in WSD of 49.66, 42.84, and 40.24%, respectively. Same goes to COF, B40 also has the lowest WSD among quaternary fuel because of higher biodiesel component that improve the viscosity of the blend. In addition, higher composition of PPO and WCB in the quaternary fuels reduces the wear. According to Table VII, the present study reported that WSD exhibits the same pattern with previous studies, in which biodiesel and PPO result in lower WSD than diesel.

< ***Insert Figure 4*** >

Figure 4 Average WSD for all tested fuel samples by HFRR tester

SEM was used to examine the wear surface morphology of steel plates, and the scar worn surface images are displayed in Figure 5. The findings show that all of the fuel samples examined had significant surface deformations. Adhesive wear, tribo-oxidation, creaks and cracks on the metal surface of B30a, B20, B10, and B30b were discovered. Grooves were only discovered on the metal surface of B20. A similar observation was made on diesel fuel by Azad *et al.* (2018), who looked at the lubricating properties of ternary fuel blends. Based on the surface morphology, the balls removed the metal layers from the worn surface of their sliding direction, as shown Figure 5. Adhesive wear was detected on the sliding surfaces due to the increased wear debris particle size. Surface damage of more than 20 μm was measured, implying this effect.

< ***Insert Figure 5*** >

Figure 5 SEM worn surface images at 500 (left), 2000 (middle), and 3000× (right) magnification: (a, a', a") B10, (b, b', b") B30a, (c, c', c") B20, (d, d', d") B30a, and (e, e', e") B40

The oxidative corrosion caused by various fatty acids was illustrated by the black areas on the worn surfaces (Awang *et al.*, 2020). The oxidation process converts the esters into fatty acids such as formic acid, acetic acid, propionic acid, caproic acid, and others (Fazal *et al.*, 2013). The inclusion of polyunsaturated fatty acids in PB, such as oleic acid (Table I) , could be the most influential factor in auto-oxidation (Fazal *et al.*, 2013). The presence of fatty acids in PB caused corrosive oxidation, according to Table I. When PPO percentage in fuel blends increased from 5 (B20) to 15% (B40), corrosive oxidation decreased due to the low concentration of fatty acid and reduced oxidative corrosion.

Furthermore, B10 was found to have more creaks than quaternary fuels and B30a. This is due to its lower viscosity, which results in a thinner protective layer. B40 produced a smoother overall surface finish than B20 and B30b because of the polishing action of PPO (Awang *et al.*, 2020). An identical observation was made by Awang *et al.* (2020). They claimed that increasing amount of PPO in the fuel blends improved the surface finish. Furthermore, higher oxygen concentrations induced by WCB resulted in the creation of additional metal oxides, increasing the lubricating layer on the sliding surface. As a result, friction and wear between the contact surfaces were reduced for B40.

## 4. Conclusions

The effects of PPO and WCB in the PB-diesel mixture on lubricating properties during injection applications in diesel engines were the focus of this tribological study. All fuel samples are evaluated using HFRR equipment to determine lubricity in compliance with the ASTM D6079 standard method.

The percentage of unsaturated fatty acids is more in POB (49.52%) compared to WCB (35.94%). This unsaturated portion of fatty acids in the biodiesel increases the lubricity of blended fuel. PPO has a lower alkane content than that of B10, leading to lower viscosity of PPO. Therefore, it is suitable for injection with diesel in diesel engines. The kinematic viscosity and density of B30b quaternary fuels were lower than that of B30a binary fuel. B10 showed the lowest lubricity compared to other fuel samples due to it high values of COF and WSD as well as more surface deformations. The COF and WSD of all quaternary fuel mixes were lower than B10 (commercial diesel). In comparison to B10, B30a showed a 9.3% increase in WSD. The different acids created when the esters in PB are oxidized cause this effect, which is known as oxidative corrosion. Meanwhile, as compared to B30a, the quaternary fuel mixes (B40, B30b, and B20) exhibit a reduction in WSD of 49.66, 42.84, and 40.24%, respectively.

In comparison to B30a, B30b exhibits a 22.34% increase in COF. For future study, the additives such as nanoparticles or oxidised alcohol can be added in quaternary fuels to improve lubricity properties, resulting in decreased COF when compared to blank quaternary fuels. Because the nanoparticles serve as a sacrificial layer between the rubbing surfaces, this is the case. Among the quaternary fuels, B40 exhibited the best overall lubricating performance, which was confirmed by surface morphology analysis. B40 had the greatest COF and WSD reductions of 7.63 and 44.5%, respectively, followed by B30b and B20. B40 also has the least adhesive wear and tribo-oxidation than B20 and B30b. B40 produced a smoother overall surface finish than B20 and B30b due to the polishing action of PPO.

It is proven that the addition of PPO and WCB into PB-diesel blend improves the durability of diesel engines, pumps, and fuel injectors because they improve the lubricity of PB-diesel fuel.

**Acknowledgements**

The authors take the opportunity to thank Universiti Malaya for the financial support under research grant IIRG008B-2019 under Universiti Malaya Impact-Oriented Interdisciplinary Research Grant Programme.

**References**

Abed, K., El Morsi, A. K., Sayed, M. M., El Shaib, A., and Gad, M. (2018), "Effect of waste cooking-oil biodiesel on performance and exhaust emissions of a diesel engine", *Egyptian Journal of Petroleum*, Vol. 27 No. 4, pp.985-989.

Abu Jrai, A., Yamin, J., Al-Muhtaseb, A. a., and Hararah, M. (2011), "Combustion characteristics and engine emissions of a diesel engine fueled with diesel and treated waste cooking oil blends", *Chemical Engineering Journal*, Vol. 172, pp.129-136.

Agarwal, A. (2003), "Lubricating oil tribology of a biodiesel-fuelled compression ignition engine", In Internal Combustion Engine Division Spring Technical Conference, Vol. 36789, pp.751-765.

Al-Dawody, M. F., Jazie, A. A., and Abbas, H. A. (2019), "Experimental and simulation study for the effect of waste cooking oil methyl ester blended with diesel fuel on the performance and emissions of diesel engine", *Alexandria Engineering Journal*, Vol. 58 No. 1, pp.9-17.

Ali, O. M., Mamat, R., Abdullah, N. R., and Abdullah, A. A. (2016), "Analysis of blended fuel properties and engine performance with palm biodiesel–diesel blended fuel", *Renewable Energy*, Vol. 86, pp.59-67.

An, H., Yang, W. M., Maghbouli, A., Li, J., Chou, S. K., and Chua, K. J. (2013), "Performance, combustion and emission characteristics of biodiesel derived from waste cooking oils", *Applied Energy*, Vol. 112, pp.493-499.

Antelava, A., Damilos, S., Hafeez, S., Manos, G., Al-Salem, S. M., Sharma, B. K., Kohli, K. and Constantinou, A. (2019), "Plastic Solid Waste (PSW) in the Context of Life Cycle Assessment (LCA) and Sustainable Management", *Environmental Management*, Vol. 64 No. 2, pp.230-244.

Awang, M. S. N., Zulkifli, N. W., Abbas, M. M., Zulkifli, S. A., Kalam, M. A., Ahmad, M. H., Yusoff, M. N. A. M., Mazlan, M. and Daud, W. M. A. W. (2021), "Effect of Addition of Palm Oil Biodiesel in Waste Plastic Oil on Diesel Engine Performance, Emission, and Lubricity", *ACS Omega*.

Awang, M. S. N., Zulkifli, N. W. M., Abbas, M. M., Zulkifli, S. A., Yusoff, M. N. A. M., Ahmad, M. H., and Daud, W. M. A. W. (2020), "Effect of blending local plastic pyrolytic oil with diesel fuel on lubricity", *Jurnal Tribologi*, Vol. 27, pp.143-157.

Azad, A. K., Rasul, M. G., Sharma, S. C., and Khan, M. M. K. (2018), "The Lubricity of Ternary Fuel Mixture Blends as a Way to Assess Diesel Engine Durability", *Energies*, Vol. 11 No. 1, pp.33.

Czajczyńska, D., Anguilano, L., Ghazal, H., Krzyżyńska, R., Reynolds, A. J., Spencer, N., and Jouhara, H. (2017), "Potential of pyrolysis processes in the waste management sector", *Thermal Science and Engineering Progress*, Vol. 3, pp.171-197.

Dhar, A., and Agarwal, A. (2014), "Experimental investigations of effect of Karanja biodiesel on tribological properties of lubricating oil in a compression ignition engine", *Fuel*, Vol. 130, pp.112–119.

Elisha, O., Fauzi, A., and Anggraini, E. (2019), "Analysis of Production and Consumption of Palm-Oil Based Biofuel using System Dynamics Model: Case of Indonesia", *International Journal of Engineering, Science and Technology*, Vol. 6.

Fazal, M. A., Haseeb, A. S. M. A., and Masjuki, H. H. (2013), "Investigation of friction and wear characteristics of palm biodiesel", *Energy Conversion and Management*, Vol. 67, pp.251-256.

Gad, M., Abu-Elyazeed, O., Mohamed, M., and Hashim, A. (2021), "Effect of oil blends derived from catalytic pyrolysis of waste cooking oil on diesel engine performance, emissions and combustion characteristics", *Energy*, Vol. 223, pp.120019.

Gardy, J., Nourafkan, E., Osatiashtiani, A., Lee, A. F., Wilson, K., Hassanpour, A., and Lai, X. (2019), "A core-shell SO4/Mg-Al-Fe3O4 catalyst for biodiesel production", *Applied Catalysis B: Environmental*, Vol. 259, pp.118093.

Gopal, K. N., Mana, A. P. and Ashok, B. (2018), "Tribological characteristics of Pongamia oil methyl ester", *Jurnal Tribologi,* Vol. 17, pp.65-76.

Hu, X., Wang, X., Chen, J., Xu, Y., & Hu, E. (2016), "Tribological behavior of diesel/biodiesel blend from waste cooking oil and ethanol", *Energy Sources, Part A: Recovery, Utilization, and Environmental Effects*, Vol. 38 No. 8, pp.1062-1067.

Jamshaid, M., Masjuki, H. H., Kalam, M. A., Mohd Zulkifli, N. W., Ahmed, A., and Zulfattah, Z. M. (2020), "Effect of Fatty Acid Methyl Ester on Fuel-Injector Wear Characteristics", *Journal of Biobased Materials and Bioenergy*, Vol. 14, pp.327-339.

Juwono, H., Fauziah, L., Uyun, I.Q., Alfian, R., Suprapto, Ni'mah, Y.L. and Ulfin, I. (2018), "Catalytic convertion of Al-MCM-41-ceramic on hidrocarbon (C8 – C12) liquid fuel synthesis from polypropylene plastic waste", *AIP Conference Proceedings*, Vol. 2049 No. 1, pp.020080.

Kaewbuddee, C., Sukjit, E., Srisertpol, J., Maithomklang, S., Wathakit, K., Klinkaew, N., Liplap, P. and Arjharn, W. (2020),"Evaluation of Waste Plastic Oil-Biodiesel Blends as Alternative Fuels for Diesel Engines", *Energies*, Vol. 13, pp.2823.

Kalargaris, I., Tian, G., and Gu, S. (2017), "Experimental evaluation of a diesel engine fuelled by pyrolysis oils produced from low-density polyethylene and ethylene–vinyl acetate plastics", *Fuel Processing Technology*, Vol. 161, pp.125-131.

Kulkarni, M. G., Dalai, A. K., and Bakhshi, N. N. (2007), "Transesterification of canola oil in mixed methanol/ethanol system and use of esters as lubricity additive", *Bioresource Technology*, Vol. 98, No. 10, pp.2027-2033.

Latiff, R. (2020), "Malaysia to implement B30 biodiesel mandate in transport sector before 2025", Sarkar, H., Ed.

Moecke, E., Feller, R., Santos, H., Machado, M., Cubas, A., Dutra, A., A.R., Santos, L.L.V. and Soares, S. (2016), "Biodiesel production from waste cooking oil for use as fuel in artisanal fishing boats: Integrating environmental, economic and social aspects", *Journal of Cleaner Production*, Vol. 135. pp.679-688.

Mohamed, R. M., Kadry, G. A., Abdel-Samad, H. A., and Awad, M. E. (2020), "High operative heterogeneous catalyst in biodiesel production from waste cooking oil", *Egyptian Journal of Petroleum*, Vol. 29 No. 1, pp.59-65.

Mujtaba, M. A., Masjuki, H. H., Kalam, M. A., Noor, F., Farooq, M., Ong, H. C., Gul, M., Soudagar, M.E.M., Bashir, S., Rizwanul Fattah, I.M. and Razzaq, L. (2020), "Effect of Additivized Biodiesel Blends on Diesel Engine Performance, Emission, Tribological Characteristics, and Lubricant Tribology", *Energies*, Vol. 13 No. 13, pp.3375.

Pehan, S., Jerman, M. S., Kegl, M., and Kegl, B. (2009), "Biodiesel influence on tribology characteristics of a diesel engine", *Fuel*, Vol. 88 No. 6, pp.970-979.

Razzaq, L., Mujtaba, M., Soudagar, M. E. M., Ahmed, W., Fayaz, H., Bashir, S., Fattah, I.R., Ong, H.C., Shahapurkar, K., Afzal, A. and Afzal, A. (2021), "Engine performance and emission characteristics of palm biodiesel blends with graphene oxide nanoplatelets and dimethyl carbonate additives", *Journal of environmental management*, Vol. 282, pp.111917.

Sachuthananthan, B., Reddy, D., Mahesh, C., and Dineshwar, B. (2018), "Production of diesel like fuel from municipal solid waste plastics for using in CI engine to study the combustion, performance and emission characteristics", *Indian Journal of Pure and Applied Mathematics*, Vol. 119, pp.85-96.

Sikdar, S., Siddaiah, A., and Menezes, P. (2020), "Conversion of Waste Plastic to Oils for Tribological Applications", *Lubricants*, Vol. 8 No. 8, pp.78.

Singh, T. S., Rajak, U., Dasore, A., Muthukumar, M., and Verma, T. N. (2021), "Performance and ecological parameters of a diesel engine fueled with diesel and plastic pyrolyzed oil (PPO) at variable working parameters", *Environmental Technology & Innovation*, Vol. 22, pp.101491.

Sudrajat, A., Tamaldin, N., Yamin, A. K. M., Bin, M. F., Tunggal, D. and Chichiri, B. (2020), "Performance analysis of biodiesel engine by addition of HHO gas as a secondary fuel", *Jurnal Tribologi,* Vol. 26, pp.120-134.

Wadumesthrige, K., Ara, M., Salley, S. O., and Ng, K. Y. S. (2009), "Investigation of Lubricity Characteristics of Biodiesel in Petroleum and Synthetic Fuel", *Energy & Fuels*, Vol. 23 No. 4, pp.2229-2234.

Wain, K. S., Perez, J. M., Chapman, E., and Boehman, A. L. (2005), "Alternative and low sulfur fuel options: boundary lubrication performance and potential problems", *Tribology International*, Vol. 38 No. 3, pp.313-319.

Yusuff, A. S., Bhonsle, A. K., Trivedi, J., Bangwal, D. P., Singh, L. P., and Atray, N. (2021), "Synthesis and characterization of coal fly ash supported zinc oxide catalyst for biodiesel production using used cooking oil as feed", *Renewable Energy*, Vol. 170, pp.302-314.

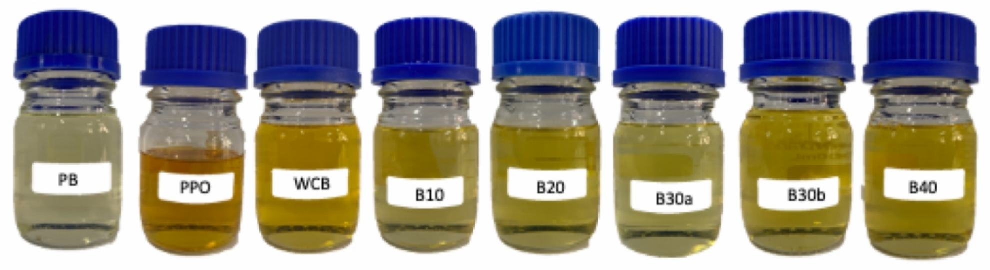


Figure 1 Tested blank fuels and quaternary fuel blends

139x38mm (300 x 300 DPI)

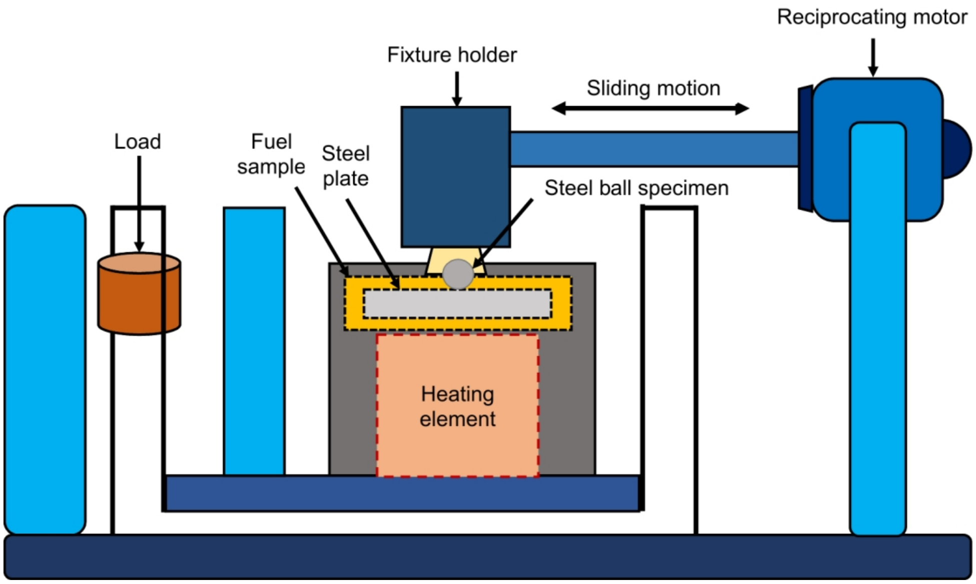


Figure 2 Schematic view of reciprocating friction and wear monitor (HFRR) rig

142x83mm (300 x 300 DPI)

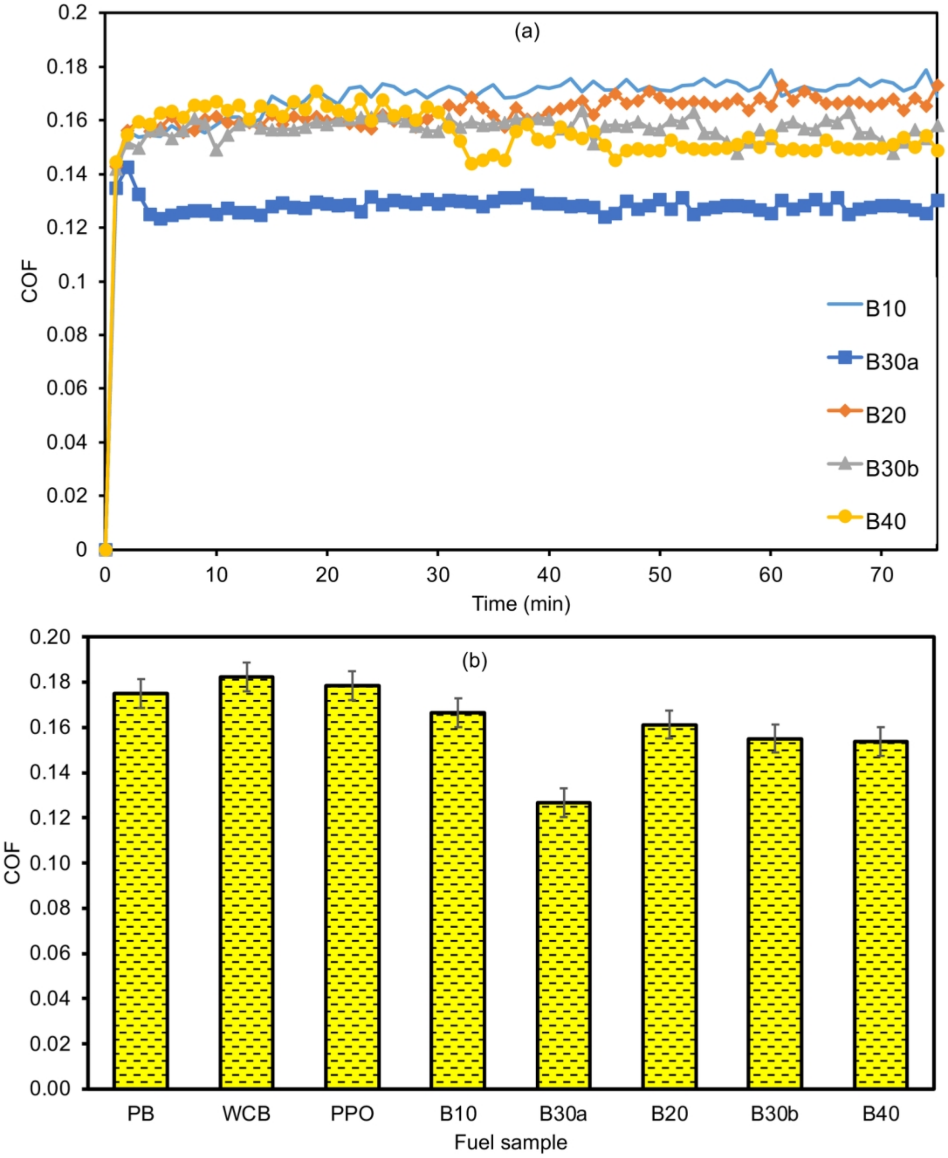


Figure 3 (a) COF during the run-in period and steady-state period and (b) average COF for all tested fuel samples by HFRR tester

298x365mm (150 x 150 DPI)

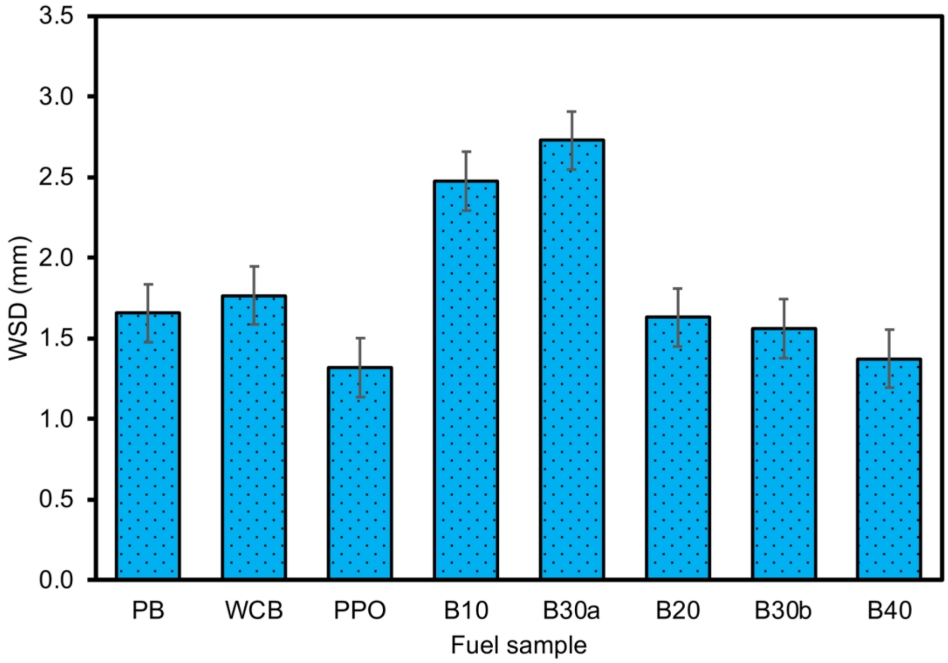


Figure 4 Average WSD for all tested fuel samples by HFRR tester

316x215mm (150 x 150 DPI)

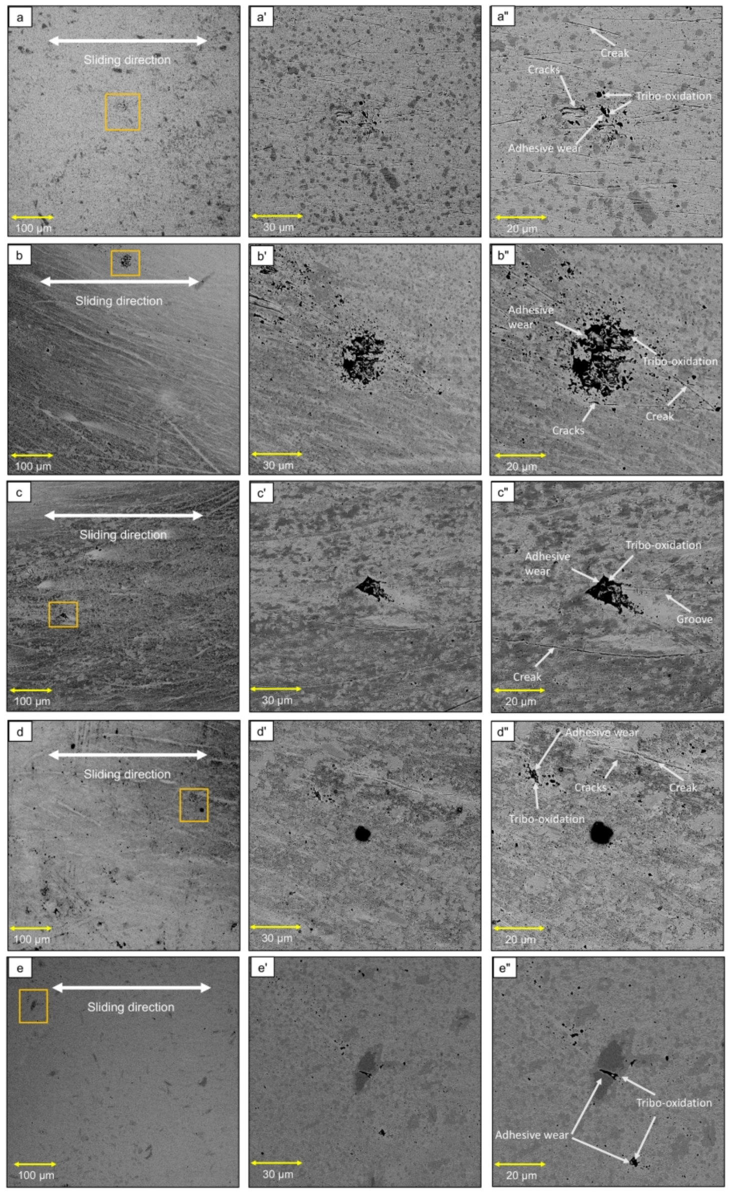


Figure 5 SEM worn surface images at 500 (left), 2000 (middle), and 3000× (right) magnification: (a, a’, a”) B10, (b, b’, b”) B30a, (c, c’, c”) B20, (d, d’, d”) B30a, and (e, e’, e”) B40

330x522mm (150 x 150 DPI)

Table I Chemical composition of PB, WCB and B10

| Fatty acid | | Structure | Area (%) | | |
|---|---|---|---|---|---|
| Common name | Formal name | | PB | WCB | B10 |
| Caprylic acid | Octanoic acid | C8:0 | 0.34 | 2.39 | - |
| Capric acid | Decanoic acid | C10:0 | 0.10 | 0.37 | - |
| Lauric acid | Dodecanoic acid | C12:0 | 1.28 | 1.96 | - |
| Myristic Acid | Tetradecanoic acid | C14:0 | 4.79 | 5.17 | 0.8 |
| Pentadecanoic acid | Pentadecanoic acid | C15:0 | 0.29 | 0.84 | - |
| Palmitic acid | Hexadecanoic acid | C16:0 | 34.74 | - | 2.09 |
| Heptadecanoic acid | Heptadecanoic acid | C17:0 | 0.58 | - | - |
| Oleic acid | cis-9-Octadecenoic acid | C18:1 | 48.45 | - | - |
| Linolenic acid | cis-9,12,15-Octadecatrienoic acid | C18:3 | - | 2.89 | - |
| Arachidic acid | Eicosanoic acid | C20:0 | - | - | 0.43 |
| Gondoic acid | cis-11 Eicosenoic acid | C20:1 | 1.07 | 33.05 | - |
| Lignoceric acid | Tetracosanoic acid | C24:0 | 1.23 | - | - |
| Total saturated fatty acids | | | 43.35 | 10.73 | 3.32 |
| Total unsaturated fatty acids | | | 49.52 | 35.94 | - |

Table II The composition of different tested quaternary fuel blends

| Sample Code | Fuel composition (by volume) |
|---|---|
| B10 | 90% diesel and 10% PB |
| B30a | 70% diesel and 30% PB |
| B20 | 80% diesel, 10% PB, 5% PPO and 5% WCB |
| B30b | 70% diesel, 10% PB, 10% PPO and 10% WCB |
| B40 | 60% diesel, 10% PB, 15% PPO and 15% WCB |

Table III Physicochemical properties of tested fuel blends

| Properties of test fuel | Test method | PB | PPO | WCB | B10 | B30a | B20 | B30b | B40 |
|---|---|---|---|---|---|---|---|---|---|
| Density at 15 ˚C (kg/m$^3$) | ASTM D4052 | 0.9360 | 0.7903 | 0.8840 | 0.8482 | 0.8534 | 0.8474 | 0.8446 | 0.9449 |
| Kinematic viscosity at 40 ˚C (mm$^2$/s) | ASTM D445 | 5.5932 | 1.4182 | 5.0406 | 2.7658 | 3.3093 | 2.8407 | 2.8885 | 2.868 |
| Kinematic viscosity at 100 ˚C (mm$^2$/s) | ASTM D445 | 1.7414 | 0.5991 | 1.7593 | 1.2834 | 1.3551 | 1.2805 | 1.2244 | 1.1942 |
| Dynamic viscosity at 40 ˚C (mPa.s) | ASTM D445 | 3.9642 | 0.8537 | 3.8872 | 2.6453 | 2.8400 | 2.5468 | 2.4345 | 2.3407 |
| Dynamic viscosity at 100 ˚C (mPa.s) | ASTM D445 | 1.4158 | 0.4330 | 1.4458 | 1.0107 | 1.0337 | 1.0067 | 0.9612 | 0.9363 |
| Viscosity index | ASTM D2270 | 183.9 | 76.3 | 226.3 | 154.3 | 163.6 | 226.3 | 203.4 | 233.4 |
| Calorific value (MJ/kg) | ASTM D240 | 44.20 | 42.70 | 39.77 | 44.70 | 43.82 | 43.15 | 43.17 | 42.57 |
| Flash point (˚C) | ASTM D93 | 174 | 47 | 192 | 80 | 89 | 73 | 68 | 64 |
| Oxidation stability at 110 ˚C (induction time/hr) | ASTM D7462 | 3.96 | 42.76 | 2.81 | - | 23.02 | 23.80 | 12.28 | 7.49 |

Table IV HFRR tribological test operating conditions

| Test parameters | Standard value |
|---|---|
| Sample temperature | 25 °C |
| Sample test duration | 75 min |
| Applied load | 2 N |
| Frequency | 50 Hz |
| Stroke length | 1 mm |
| Sample volume | 2 ml |

Table V GC-MS composition of B10

| Retention Time (min) | Composition (%) | Compound | Retention time (min) | Composition (%) | Compound |
|---|---|---|---|---|---|
| 11.878 | 1.14 | Dodecane | 24.862 | 2.23 | Heptadecane |
| 13.883 | 1.37 | 4-methyldecane | 25.057 | 1.05 | 2,6,10,14-tetramethyl-pentadecane |
| 14.714 | 1.04 | Tridecane | 27.054 | 2.60 | Hexadecane |
| 16.75 | 1.23 | 4,6-dimethyldodecane | 27.855 | 1.41 | Heptadecane |
| 17.477 | 3.06 | Hexadecane | 29.207 | 3.02 | Heptadecane |
| 19.043 | 2.19 | Hexadecane | 29.687 | 2.9 | Hexadecanoic acid methyl ester |
| 20.018 | 2.67 | Hexadecane | 31.177 | 2.05 | Heptadecane |
| 20.851 | 1.68 | 2,3,6-trimethylnaphthalene | 31.843 | 1.08 | Heneicosane |
| 21.558 | 1.62 | 4-methyltetradecane | 33.399 | 1.00 | Heneicosane |
| 22.477 | 2.63 | Hexadecane | 34.939 | 1.42 | Heneicosane |
| 23.623 | 2.75 | Hexadecane | 36.675 | 1.18 | Eicosane |

Table VI GC-MS composition of PPO

| Retention Time (min) | Composition (%) | Compound | Retention time (min) | Composition (%) | Compound |
|---|---|---|---|---|---|
| 5.673 | 1.04 | 1,2,4-trimethylbenzene | 22.175 | 3.15 | 1-tetradecene |
| 6.001 | 2.59 | Methylstyrene | 22.427 | 5.23 | Hexadecane |
| 11.71 | 2.69 | 1-dodecene | 23.627 | 1.35 | 1,1'-(1,3-propanediyl)bis-benzene |
| 12.833 | 1.08 | 4,6-dimethyldodecane | 23.635 | 1.29 | 1,1'-(1,3-propanediyl)bis-benzene |
| 14.957 | 2.53 | 7-methylundecene | 24.737 | 2.96 | Heptadecane |
| 17.187 | 4.34 | 1-tetradecene | 26.92 | 2.52 | Heptadecane |
| 17.43 | 5.63 | Hexadecane | 29.005 | 2.37 | Heneicosane |
| 18.914 | 1.23 | Heptadecane | 30.99 | 1.88 | Eicosane |
| 19.104 | 1.08 | Hexadecane | 32.883 | 1.52 | Heneicosane |
| 19.738 | 4.20 | 1-tridecene | 34.711 | 1.00 | Heneicosane |

Table VII A brief comparison of COF and WSD resulted from present study with other research works

| **Fuel sample** | **Composition** | **Reference fuel** | **COF (%)** | **WSD (%)** | **Reference** |
|---|---|---|---|---|---|
| B40 | 60% diesel +10% PB +15% PPO +15% WCB | Commercial diesel | ↓ 7.63 | ↓ 44.5 | Current study |
| B30 | 30% PB + 70% diesel | | ↓11.63 | NA | Razzaq *et al.* (2021) |
| B50 | 50% PB + 50% diesel | | ↓ 3.74 | ↓12.18 | Fazal *et al.* (2013) |
| POME50 | 50% PB + 50% diesel | | ↓ 13.90 | NA | Jamshaid *et al.* (2020) |
| CPME50 | 25% castor oil biodiesel +25% PB and 50% diesel | | ↓ 10.4 | NA | |
| PO10 | 10% PPO, 90% diesel | | ↓ 16.06 | ↓ 17.96 | Awang *et al.* (2020) |
| B30 | 30% palm-sesame oil biodiesel + 70% diesel | | ↓ 31.10 | ↓ 43.27 | Mujtaba *et al.* (2020) |

NA: not available